Rapid nitrification of wastewater ammonium near coastal ocean outfalls, Southern California, USA

McLaughlin, Karen[1,*], Nikolay P. Nezlin[1], Meredith D.A. Howard[1], Carly D.A. Beck[1], Raphael M. Kudela[2], Michael J. Mengel[3], George L. Roberston[3]

[1]Southern California Coastal Water Research Project, Costa Mesa, CA

[2]University of California, Santa Cruz, CA

[3]Orange County Sanitation District, Fountain Valley, CA

[*]Corresponding Author, karenm@sccwrp.org, 714-755-3242

Keywords: Southern California Bight, anthropogenic nutrients, wastewater, nitrification, nitrogen cycling, stable isotopes.

Abstract

In the southern California Bight (SCB), there has been a longstanding hypothesis that anthropogenic nutrient loading is insignificant compared to the nutrient loading from upwelling. However, recent studies have demonstrated that, in the nearshore environment, nitrogen (N) flux from wastewater effluent is equivalent to the N flux from upwelling. The composition of the N pool and N:P ratios of wastewater and upwelled water are very different and the environmental effects of wastewater discharges on coastal systems are not well characterized. Capitalizing on routine maintenance of the Orange County Sanitation District's ocean outfall, wherein a wastewater point source was "turned off" in one area and "turned on" in another for 23 days, we were able to document changes in coastal N cycling, specifically nitrification, related to wastewater effluent. A "hotspot" of ammonium (NH_4^+) and nitrite (NO_2^-) occurred over the ocean outfall under normal operations and nitrification rates were significantly higher offshore when the deeper outfall pipe was operating. These rates were sufficiently high to transform all effluent NH_4^+ to nitrate (NO_3^-). The dual isotopic composition of dissolved NO_3^- ($\delta^{15}N_{NO3}$ and $\delta^{18}O_{NO3}$) indicated that N-assimilation and denitrification were low relative to nitrification, consistent with the relatively low chlorophyll and high dissolved oxygen levels in the region during the study. The isotopic composition of suspended particulate organic matter (POM) recorded low $\delta^{15}N_{PN}$ and $\delta^{13}C_{PN}$ values around the outfall under normal operations suggesting the incorporation of "nitrified" NO_3^- and wastewater dissolved organic carbon into POM. Our results demonstrate the critical role of nitrification in nitrogen cycling in the nearshore environment of urban oceans.

1. Introduction

Nitrogen (N) pollution is considered to be one of the greatest consequences of human-accelerated global change on coastal oceans (Howarth and Marino 2006). However, in upwelling dominated systems such as the Southern California Bight (SCB), there has been a general perception that the flux of anthropogenic nutrient inputs is insignificant relative to upwelling flux, and therefore anthropogenic inputs have relatively little effect on the productivity of coastal waters (Chavez and Messié 2009, Capone and Hutchins 2013). Recent studies in the SCB have shown that, in nearshore regions associated with high urbanization, N loads from wastewater effluent are roughly equivalent to nutrient loads from upwelling (Howard et al. 2014). This has effectively doubled the N loading to the shelf, potentially altering the composition of the N pool (effluent N is primarily ammonium, upwelled N is primarily nitrate) as well as the nitrogen: phosphorus (N:P) ratio (P discharges are low relative to N; effluent N:P ~115). The effect of these discharges on nearshore biological community composition and nutrient cycling is largely unknown.

There is an emerging body of circumstantial evidence suggesting that terrestrial, anthropogenic nutrients, dominated by wastewater effluent, are having an effect on primary productivity and respiration in Southern California coastal waters. In particular, increased nearshore primary productivity and the spatial extent and duration of algal blooms have increased over the past decade (Nezlin et al. 2012). Furthermore, respiration of high levels of organic matter from algal blooms may be contributing to observations of reduced coastal dissolved oxygen concentrations relative to offshore trends (Booth et al. 2014). However, the

extent and magnitude of increased productivity and respiration, particularly that which is supported by wastewater nutrients, relative to baseline production in the SCB is still uncertain.

The San Pedro Shelf in the SCB is an ideal place to study the fate of wastewater ammonium in urban coastal waters. Two of the four major Publicly Owned Treatment Works (POTW) in the SCB discharge wastewater on the San Pedro Shelf and these outfalls make up to 50% of all of the POTW discharges in the SCB (Howard et al. 2012). In addition, between 1971 and 2000, the effluent volume discharged to the SCB increased by 31% and N emissions increased 91% (Lyon and Stein 2009). For this study, we took advantage of planned maintenance of the Orange County Sanitation District's (OCSD) effluent outfall pipes. For three weeks in the fall of 2012, OCSD diverted its effluent stream (138 million gallons of wastewater per day) from its deeper outfall to its shallower outfall while the latter was cleaned and repaired. This diversion provided a unique opportunity to conduct an *in situ* experiment (normally prohibited by regulatory requirements) to directly document the effects of turning off a wastewater point source in one area and turning it on in another. We focus on the effect of wastewater N because the SCB is largely N limited (Thomas et al. 1974, Cullen and Eppley 1981) and the wastewater contains high levels of nitrogenous species. Because effluent N is primarily ammonium and previous observations in the SCB have indicated the ammonium is a minor N species despite the large ammonium-dominated wastewater discharges (Howard et al. 2012), we hypothesized that wastewater ammonium is rapidly nitrified near POTW outfalls.

To understand the fate of effluent N, we employed stable isotope techniques to trace dissolved nitrate, ammonium, and particulate organic matter; we also determined rates of

nitrification of ammonium, the dominant N form in effluent. The stable isotopic compositions

of dissolved nitrate ($\delta^{15}N_{NO3}$ and $\delta^{18}O_{NO3}$) and suspended particulate matter ($\delta^{15}N_{PN}$ and $\delta^{13}C_{PN}$)

are natural tracers of N sources and cycling in the ocean. Variation in the isotopic composition

is attributable to distinct source signatures and the mass dependent isotopic discriminations

associated with various biogeochemical transformations that constitute the marine N cycle.

Because each pathway causes a characteristic shift in isotope composition of the products and

reactants, the isotopic composition of the dissolved and particulate pools can provide useful

information on the mechanism of these transformations (Sigman et al. 2005, Wankel et al.

2007, Sugimoto et al. 2009).

2. Materials and Methods

2.1. Field Collection.

The OCSD discharges wastewater from its treatment facility in Huntington Beach,

California offshore via one of two outfall pipes located on the San Pedro Shelf in Southern

California. Normal operations require OCSD to discharge effluent from its deeper outfall

located 7 km off shore and in 56 meters of water depth (33°34.5'N; 118°00.5'W), hereafter

referred to as "deep outfall"; however, during maintenance of the deep outfall, wastewater

was diverted to OCSD's secondary outfall pipe located 1.6 km offshore in 16.7 meters water

depth (33°36.8'N; 117°58.5'W), hereafter referred to as "shallow outfall". Wastewater was

diverted from 11 September 2012 until 3 October 2012. Sampling was conducted pre-diversion

(6 September 2012), two weeks into the diversion (20 September 2012), shortly after the

diversion ended (less than 24 hours), hereafter called transition (3 October 2012), and two

weeks post-diversion (17 October 2012). Sampling cruises on 6 Sep and 20 Sep were conducted aboard the *R/V Yellowfin* and cruises on 3 Oct and 17 Oct were conducted on the *M/V Nerissa*.

Sampling was conducted at stations along an across shelf transect from the shallow outfall pipe past the deep outfall to the offshore stations (Figure 1). Vertical profiles were collected at each station using a package containing a SBE911plus (Seabird Electronics, Inc.) conductivity-temperature-depth (CTD) profiler with a chlorophyll sensor and a colored dissolved organic matter (CDOM) sensor; however the CDOM sensor aboard the *R/V* Yellowfin failed quality assurance tests and, thus, data from that sensor was rejected for cruises on 6 Sep and 20 Sep.

Discrete samples were collected from Niskin bottles (1.5 and 3 Liter) on a rosette deployed with the sensor package. Samples were collected at three depths at each station: surface, deep chlorophyll maximum (12 - 30 m), and below the mixed layer ("subeuphotic", 30 - 75 m). Sampling was adaptive at each site, with sample depths determined by downcast observations of chlorophyll (to determine the layer of maximum chlorophyll fluorescence) and temperature, salinity and CDOM (to determine the below mixed layer depth that fell within the plume track). The "subeuphotic" samples (the deepest samples collected) from the periods when effluent was discharged from the deep outfall were collected within the center of the plume track directly over the outfall (at station 2205). However, because the plume-track rose just below the euphotic zone as it moved offshore, subeuphotic samples at the offshore stations were collected below the center of the plume track, in more effluent-diluted waters, to minimize photoinhibition of nitrification. All samples were transferred from the Niskins using

acid-washed Tygon tubing into acid-washed 2 L high density polyethylene (HDPE) bottles that were triple rinsed with sample water before filling. Sub-samples for nutrient and nitrate stable isotope analysis were vacuum filtered through a 0.45 µM polycarbonate filter (Millipore) and collected in triple-rinsed, 60 mL HDPE amber bottles, stored on ice for transport to the laboratory, and frozen until analysis (Wankel et al. 2006, Wankel et al. 2007, Santoro et al. 2010a). Samples for ammonium stable isotope analysis were vacuum filtered through a 0.45 µM polycarbonate filter (Millipore), collected into triple-rinsed, 2 L HDPE bottle, acidified with several drops of concentrated ammonia-free sulfuric acid to a pH less than 2 and stored on ice for transport, and kept at 4 °C until analysis (Holmes et al. 1998). Samples for nitrification rate incubations were collected directly into acid washed, triple-rinsed, 2 L HDPE bottles and stored on ice in the dark until the incubations could begin in the laboratory within six hours of collection.

Suspended particulate and net tow samples were collected by vacuum filtration onto pre-combusted (450 °C for 4 hours) glass fiber filters (Whatman GF/F). Suspended particulate samples were sub-sampled from the same whole water sample collected for nutrient and stable isotope analyses. Net tow samples were collected by lowering both a 20 µm and 200 µm net through the water column 3 times to 10 m to generate a composite sample of the plankton communities. Tow samples were collected into a 1L HDPE bottle prior to filtration. Filters were collected into snap-close petri dishes and stored in Ziploc bags on ice in the dark for transport. Filters in the petri dishes were dried at 50 °C in the dark until analysis.

OCSD supplied samples of effluent for analysis prior to each sampling event. These samples were collected as a composite over 24 hours in an acid washed 1 L HDPE bottle. Effluent was stored at 4 °C while the composite was generated. The composite was subsampled into HDPE bottles and hand-filtered through 0.45 µM polycarbonate filter (Millipore) for nutrient concentrations, nitrate dual isotope analysis, and was acidified for ammonium stable isotope analysis.

2.2. Laboratory Analyses.

Nutrient concentrations. Discrete samples were analyzed for a suite of dissolved nutrients. Nitrate + nitrite, soluble reactive phosphate, and ammonium were analyzed using flow injection analyses (FIA, Lachat Instruments, QuikChem 8000 at the Marine Science Institute, at the University of California, Santa Barbara); urea and ammonium were measured manually following the protocols of (Goeyens 1998, Holmes et al. 1999) respectively; total N (TN) and phosphorus (TP) samples were analyzed following persulfate digestion (Patton and Kryskalla 2003) using FIA. A relative assessment of nutrient limitation, N*, was also calculated, which represents the deviation in "Redfield" nitrogen: phosphorus stoichiometry due to additional sources and sinks of nitrate (Deutsch et al. 2001):

$$N* = [NO_3^-] - (16 * [PO_4^{3-}]) + 2.9 \qquad \text{(Eq 1).}$$

Positive N* values reflect regions with a source of nitrate (via nitrogen fixation) and negative N* reflects a sink of nitrate (due to denitrification), values near zero are consistent with "Redfieldian" assimilation and nitrification of organic matter or that source and loss terms are balanced (Gruber and Sarmiento 1997).

Stable Isotope Analyses. The preparation and isotope analysis (δ^{15}N, δ^{18}O) of dissolved

nitrate in discrete water samples was performed using a bacterial denitrification assay

(Casciotti et al. 2002). Isotope ratios of ^{15}N/^{14}N and ^{18}O/^{16}O were measured using a

ThermoFinnigan GasBench + PreCon trace gas concentration system interfaced to a

ThermoScientific Delta V Plus isotope-ratio mass spectrometer at the Stable Isotope Facility at

the University of California, Davis. Dissolved ammonium was extracted from discrete sample

water onto glass fiber filter "traps" (Holmes et al. 1998, Hannon and Böhlke 2008) and the

isotope ratios of ^{15}N/^{14}N were measured using a coupled Costech Elemental Analyzer with a

Finnigan Delta Plus Advantage in Continuous Flow Mode at the Marine Science Institute at the

University of California, Santa Barbara. The isotope ratios of ^{15}N/^{14}N and ^{13}C/^{12}C from

suspended particulate matter and from net tows collected on precombusted Whatman GF/F

were measured using a coupled Costech Elemental Analyzer with a Finnigan Delta Plus

Advantage in Continuous Flow Mode at the Marine Science Institute at the University of

California, Santa Barbara. Isotope ratios are reported relative to a standard as follows:

$$\delta^{15}N = [(^{15}N/^{14}N_{sample}/^{15}N/^{14}N_{standard})-1]*1000, \qquad \text{(Eq. 2)}$$

using the standard of N$_2$ in air;

$$\delta^{18}O = [(^{18}O/^{16}O_{sample}/^{18}O/^{16}O_{standard})-1]*1000, \qquad \text{(Eq. 3)}$$

using the standard of Vienna Standard Mean Ocean Water (VSMOW);

$$\delta^{13}C = [(^{13}C/^{12}C_{sample}/^{13}C/^{12}C_{standard})-1]*1000, \qquad \text{(Eq. 4)}$$

using the standard of Vienna Pee Dee Belemnite (VPDB). The standard deviation of replicate

standards for particulate material δ^{13}C was 0.084 ‰ and δ^{15}N was 0.165 ‰, and the relative

percent difference between measured standards and reference values was 0.32% and 0.88%,

respectively. The standard deviation of replicate standards for dissolved nitrate $\delta^{18}O$ was 0.17

‰ and $\delta^{15}N$ was 0.15 ‰, and the relative percent difference between measured standards and

reference values was 0.46% and 0.04%, respectively.

The relationship between $\delta^{15}N_{NO3}$ and nitrate concentration was assessed by fitting an

exponential equation of the form $y = ae^{-bx} + c$, where y is the $\delta^{15}N_{NO3}$, x is the nitrate

concentration, a and b are constants and c is the asymptotic value. The best fit curves, were

calculated by the iterative least squares estimation method. The significance of each

relationship was assessed using F-test with null-hypothesis saying that $\delta^{15}N_{NO3}$ is independent

of NO_3 (i.e., $y = \bar{y}$). It is worth mentioning that a narrow range of independent variable could

substantially obscure the observed correlations (Prairie et al. 1995), which may affect the

results.

Nitrification rate incubations: Nitrification is the sequential oxidation of NH_4^+ to NO_3^- via

NO_2^-. Nitrification rates were determined by measuring the accumulation of ^{15}N in the dissolved

nitrate pool following addition of isotopically-enriched ammonium to bottle incubations

(Santoro et al. 2010a). Water was collected from Niskins into 2 L HDPE bottles. Subsamples

from this initial sample were separated into three 500 mL acid-washed polycarbonate bottles

wrapped in black tape. An enriched (99%) tracer of $^{15}NH_4Cl$ was added to a final concentration

of 100 nM to two of the bottles and a third bottle without the tracer served as a control. Bottles

were incubated in the dark to minimize N uptake by phytoplankton and as close to *in situ*

temperature conditions as possible. Surface, euphotic zone samples were incubated in a

rigging suspended in the harbor where surface water temperature was higher than the sample

sites by 2 – 4˚C, whereas subeuphotic samples were incubated in an small refrigerator set to

the average temperature of all subeuphotic samples for each sampling period (within ± 2˚C).

For reference, Q_{10} values for nitrification are on the order of 2-3 (Henriksen 1988). Subsamples

of 50 mL each were collected at four time points (approximately 0, 12, 24, and 36 post spike

addition), syringe filtered through 0.45 μm filters and frozen until analysis for dissolved nitrate

concentration and the isotopic composition of nitrate ($\delta^{15}N_{NO3}$) as described above. Potential

nitrification rates were determined by modeling the ^{15}N and ^{14}N contents of the combined

nitrate and nitrite pool with inputs from the labeled ammonium pool and outputs through

nitrate and nitrite uptake as described in Santoro et al. (2010a). Data fitting for the ^{15}N and ^{14}N

values measured at each time point was performed using non-linear least squares regression

method using MATLAB 8.2 and Statistics Toolbox 8.3 (The MathWorks, Inc.).

3. Results

3.1. Environmental Context. Oceanic conditions throughout the study were mild, the

water column was stratified with no evidence of upwelling (Figure 2). The location of the

wastewater plume can be identified by both its CDOM and salinity signatures (Rogowski et al.

2012, Rogowski et al. 2013) (Figure 2). The location of the plume was somewhat variable in

space, located further offshore along the transect on 6 September (pre- diversion) and inshore

on 20 September (during-diversion), and centered over the deep outfall on 17 October

(transition) and 20 October (post-diversion) (Figure 2, also see Kudela et al. this issue, for

information on wastewater plume tracking during this study). Sample collection for this study

was adaptive, targeting the broader plume track, though not always within the most

concentrated portion. Progressive vector diagrams from ADCP data collected at several moored

sites demonstrated variable flow patterns, but consistent retention for at least 48 h on the shelf

within the vicinity of the outfall discharge pipes (Kudela et al. this issue).

3.2. Nutrient Concentrations. Throughout the study, ammonium concentrations and

discharge rates from the OCSD plant remained fairly constant, resulting in uniform load (Table

1, (Rogowski et al. 2014)). Based on discrete nutrient samples collected on 6 and 20 September

and 17 October, ammonium accounted for ~72% of the dissolved inorganic nitrogen, with an

elevated N:P ratio of 115:1 (molar) in the discharged effluent (Table 1). Despite the relatively

constant N-load, surface nutrient concentrations were generally low (Table 2, Figure 3a), but

not completely depleted; however, nutrient concentrations, particularly ammonium, in the

OCSD plume track were considerably higher than what has been reported for similar coastal

sites and offshore waters (Figure 3a) (Ward 1987b, Sigman et al. 2005, Santoro et al. 2010a).

Dissolved nitrate ranged from 0.01 μM to 19.8 μM, dissolved ammonium ranged from 0.02 μM

to 4.0 μM, nitrite from non-detect to 1.3 μM, and phosphate from 0.06 μM to 1.8 μM, where

lowest concentrations were near the surface and increased with depth.

Pre-diversion (6 September 2012), there was a clear "hotspot" pattern of high

ammonium and nitrite concentrations around the deep outfall (up to 4.0 μM and 0.82 μM,

respectively), which was not present during the diversion (20 September 2012) (Figure 3a) and

was a factor of 6 higher than in the far-field at the same time. Following the end of the

diversion when discharge at the deep outfall resumed (17 October 2012) elevated ammonium

concentrations in the plume track were evident again (with concentrations up to 2.5 μM),

although not as high as pre-diversion and more diffuse (Figure 3a). Interestingly, an ammonium hotspot was not observed over the shallow outfall during the diversion. Ambient nitrate concentrations were slightly, but significantly (Wilcoxon Signed Rank Test, P<0.05), elevated pre-diversion around the deep outfall relative to during the diversion.

N* values varied from slightly negative to slightly positive, suggesting there were no large additions of nitrate from nitrogen fixation or sinks due to denitrification (Figure 3a, Table 2). Negative N* values were lowest pre-diversion and in water with the lowest dissolved oxygen concentration. During diversion, N* values shift to more positive values. Following the diversion, N* values remain positive at depth.

3.3. Stable Isotope Analysis. The isotopic composition of dissolved nitrate did not significantly change following the diversion (Figures 3b and 4, Table 2). Values for $\delta^{15}N_{NO3}$ over the study period ranged from 0.88 to 10.04 ‰ and were typically higher at depth and lower at the surface for all sampling time points. Values for $\delta^{18}O_{NO3}$ ranged from 3.35 to 28.98 ‰ and were typically lower at depth and higher at the surface for all sampling time points. Subeuphotic $\delta^{15}N_{NO3}$ and $\delta^{18}O_{NO3}$ values at stations 2205 (over the deep outfall) and offshore were similar during all four sampling periods with less than 4 ‰ variability in the $\delta^{15}N_{NO3}$ and $\delta^{18}O_{NO3}$ values at these sites, whereas the nearshore, shallow station 2203 and surface samples had much greater variability in both $\delta^{15}N_{NO3}$ and $\delta^{18}O_{NO3}$. Compared to nitrate in the wastewater effluent (Table 1), environmental $\delta^{15}N_{NO3}$ values were similar to effluent (5.32 ‰), but environmental $\delta^{18}O_{NO3}$ were much higher than effluent (-4.33 ‰).

The $\delta^{15}N_{NO3}$ was related to nitrate concentration during all periods except the transition period (Figure 5, first column). At low nitrate concentrations, $\delta^{15}N_{NO3}$ was highly variable, but at higher concentrations values increased and converged to an asymptotic $\delta^{15}N_{NO3}$ value of between 7.71 ‰ and 9.14 ‰ (exclusive of the transition period). The significance of these best-fit relationships was comparatively high (Figure 5; first column). The absence of significant relationship during transition may be attributed lack of high NO_3 values measured during that period. For all time periods, except for the transition period, $\delta^{15}N_{NO3}$ increased linearly with an increasing fraction of nitrate in the DIN pool (Figure 5, second column) and decreased linearly with an increasing fraction of ammonium in the DIN pool (not shown) similar to what has been observed in other urban coastal settings (Sugimoto et al. 2009). N* was significantly, negatively correlated with $\delta^{15}N_{NO3}$ pre-diversion, but not at any other time point (Figure 5, last column).

Values of $\delta^{15}N_{NH4}$ over the deep outfall ranged from 10.36 ‰ (transition) to 11.25 ‰ (post-diversion). During the diversion, a value of 9.55 ‰ for $\delta^{15}N_{NH4}$ was recorded at depth at station 2203 near the shallow outfall (Table 2). Values for water column ammonium were slightly less than the $\delta^{15}N_{NH4}$ measured in wastewater effluent (12.78 ‰, Table 1) and higher than the average water column $\delta^{15}N_{PN}$ and $\delta^{15}N_{NO3}$ (5.28 ‰ and 6.16 ‰, respectively, Table 2).

Suspended particulate $\delta^{15}N_{PN}$ and $\delta^{13}C_{PN}$ were highly variable during the study (Table 2). The average $\delta^{15}N_{PN}$ was 5.28 ‰ and ranged from 11.05 ‰ to 1.80 ‰ and the average $\delta^{13}C_{PN}$ was -23.42 ‰ and ranged from -28.38 ‰ to -19.01 ‰. Suspended particulate $\delta^{15}N_{PN}$ and $\delta^{13}C_{PN}$ were slightly lower within the plume track pre- and post-diversion and during the transition when operation at the deep outfall resumed; $\delta^{15}N_{PN}$ values were lower over the shallow outfall

14

during the diversion (Figure 3b). Suspended particulate C:N ratios were also low, with an average C:N ratio (molar) of 4.46 and values ranging from 1.14 to 8.51; C:N ratios less than 6 are atypical of phytoplankton and characteristic of bacteria (Goldman et al. 1987). The δ^{15}N and δ^{13}C values of the 20 μM and 200 μM net tows were typically higher than the particulate material collected on a GF/F filter (by between 1 to 5 ‰ for δ^{15}N and between 0.5 and 2.5 ‰ for δ^{13}C, Figure 6).

3.4. Nitrification Rates. Nitrification rates were higher in the deepest samples (subeuphotic) during normal operations (pre- and post- diversion) compared to when the wastewater was diverted. Nitrification rates were highest at depth during all time points (Figures 3b and 7, Table 2) and were highest pre-diversion (subeuphotic zone values ranged between 72 ± 30 to 160 ± 44 nmol L^{-1} d^{-1}), dropped significantly during the diversion (23 ± 3 to 60 ± 1 nmol L^{-1} d^{-1}), and then recovered to higher rates post-diversion (15 ± 3 to 92 ± 22 nmol L^{-1} d^{-1}). Nitrification rates were highest in deeper waters offshore, rather than in the somewhat shallower waters directly over the deep outfall. Surface water rates were consistently low, typically less than 2 nmol L^{-1} d^{-1}, when detectable.

4. Discussion

4.1. Nitrification of wastewater ammonium represents a "new" source of nitrate to coastal waters.

Three lines of evidence indicate that nitrification of effluent ammonium represents a source of "new" nitrate to coastal shelves near wastewater outfalls. First and foremost were the observed rates. Pre- and post-diversion, measured rates of nitrification were higher than

during the diversion and the transition (Figure 7). Interestingly, during the diversion, nitrification rates in the surface waters were the same as during normal operation conditions (e.g., no increase in rates relative to background). This was likely because the wastewater plume was located almost exclusively in the upper 20 m of the water column (Figure 2, Kudela et al. this issue), potentially resulting in light-inhibition of nitrifying microbes or possibly inhibition from the presence of chlorination by-products in the wastewater plume (Ward 2008, Kudela et al. this issue).

The next line of evidence was the isotopic composition of dissolved nitrate, which suggested that nitrification was a large contributor to the observed isotopic composition of nitrate, and that assimilation and denitrification each played a minor role. A combination of increasing $\delta^{15}N_{NO3}$ with nitrate concentration and an increasing nitrate fraction in the DIN pool was consistent with nitrification as a main driver defining the composition of the DIN pool and the isotopic composition thereof (Sugimoto et al. 2009) (Figure 5). Nitrifying bacteria preferentially utilize ^{14}N from the NH_4^+ pool and result in a gradual enrichment from ^{14}N to ^{15}N in NO_3^- as the NH_4^+ pool is reduced (Sugimoto et al. 2009). Furthermore, while subeuphotic $\delta^{15}N_{NO3}$ and $\delta^{18}O_{NO3}$ values were similar to measured values for this area during spring upwelling periods (Howard and McLaughlin, unpublished data) and similar to values for the California Current reported by others (Sigman et al. 2005, Santoro et al. 2010b), the trajectories for $\delta^{15}N_{NO3}$ and $\delta^{18}O_{NO3}$ values from subeuphotic samples to surface samples had negative slopes (Figure 4). Thus, these trajectories were inconsistent with assimilation and denitrification, which should fall along a line with a slope of ~1 (Granger et al. 2004, Sigman et al. 2005, Wankel et al. 2007). Though, the higher $\delta^{18}O_{NO3}$ values in surface waters may reflect

16

the atmospheric deposition of N onto the SCB, which has been shown to be a relatively small, but not insignificant source of N to coastal waters (Howard et al. 2014), because atmospheric sources of nitrate have the highest recorded $\delta^{18}O_{NO3}$ (Kendall 1998). Low rates of assimilation in surface waters were consistent with observations that phytoplankton biomass was extremely low during the study period (Seegers et al. and Caron et al., this issue). This was possibly due to the presence of excessive chlorination byproducts which may have inhibited phytoplankton during the sampling period (Kudela et al., this issue); however, uptake by heterotrophic bacteria may also have been significant during the diversion (Caron et al., this issue).

The third line of evidence was the pattern in the observed nutrient concentrations. The availability of a continuous, concentrated ammonium source at the outfall would provide a rich substrate for ammonium oxidizing microbes. Indeed, within the plume track (denoted by salinity and CDOM signatures of the effluent), elevated nitrite concentrations correspond to elevated ammonium, suggesting oxidation of ammonium to nitrite. Pre- and post-diversion, nutrient concentrations, particularly ammonium, in the OCSD plume track were considerably higher than what has been reported for similar coastal sites and in offshore waters (Figure 3a, Table 2) (Ward 1987b, Sigman et al. 2005, Santoro et al. 2010a). The ammonium and nitrite "hotspots" around the deep outfall were more clearly defined pre-diversion relative to post-diversion. This was likely because post-diversion, the plume was higher in the water-column, in the euphotic zone where phytoplankton utilization may have lowered the observed concentrations, indicated by the higher concentrations of chlorophyll (Figures 2 and 3a). Pre- and post-diversion, phytoplankton communities were shown to preferentially utilize ammonium over nitrate and urea (Howard et al., this issue), thus competition for ammonium in

the euphotic zone by phytoplankton, combined with light inhibition of nitrifying bacteria, would have negatively impacted bacterial communities. Interestingly, elevated nutrient concentrations were not evident over the shallow outfall during the diversion. This may be due to rapid uptake by plankton, particularly heterotrophic bacteria, which were observed to largely increase in numbers during the diversion (Caron et al., this issue), but may also be due to a small bloom of phytoplankton in surface waters, indicated by elevated chlorophyll near the surface boil (Figure 2).

While this study was focused primarily on nitrification, we did see some evidence for denitrification, but only during the pre-diversion event. Classically, negative N* values indicate a net loss of nitrate, typically due to denitrification, and positive N* values suggest a net addition of new nitrate, typically due to the nitrification of newly fixed N (Sigman et al. 2003, Sigman et al. 2005). Pre-diversion, negative N* values were present in water with the lowest dissolved oxygen concentration, where both reduction and oxidation of nitrogen compounds may occur (Lipschultz et al. 1990). Furthermore, N* was significantly, negatively correlated with $\delta^{15}N_{NO3}$ pre-diversion (Figure 5), which may be indicative of some level of denitrification (Brandes et al. 1998). During diversion, N* values shifted to more positive values, which may be indicative of nitrification; however, we did not see an increase in nitrification rates in the surface nor at depth. However, use of N* during diversion and transition may be complicated by the large increase in heterotrophic bacteria observed (Caron et al. this issue), which would skew the expected N:P ratio. Thus, a different interpretation may be a large influx of nitrate from the remineralization of organic matter by heterotrophic bacteria. Following diversion, N*

values remain positive at depth, perhaps indicative of nitrification without denitrification, which may have been inhibited by higher dissolved oxygen concentrations.

4.2. Measured nitrification rates can account for complete conversion of wastewater ammonium.

To examine the effect of wastewater on nitrification rates, we compared the amount of ammonium oxidized in a theoretical box around the ocean outfall when the deep outfall was on versus when it was off. Nitrification rates measured during the diversion at the off-shelf stations, when the deep outfall pipe was out of service, were similar to what has been observed farther offshore in the SCB (Ward 1987a) and in Monterey Bay, CA (Ward 2005). Thus, they may represent coastal "background" nitrification rates in the absence of a wastewater plume, attributable to oxidation of ammonium from remineralized water column biomass or sediment ammonium flux. Rates measured pre- and post-diversion at the stations where the effluent plume signature is highest may represent the relative increase in nitrification due to the presence of wastewater ammonium. Current speeds over the course of the study were very slow, with water retained in the region for at least 48 hours (Kudela et al., this issue, Lucas et al., this issue), so assuming that discharged effluent ammonium remains in the vicinity of the outfall is not unreasonable. The effluent discharge rate from OCSD at the time of the diversion was approximately 5.3×10^8 liters day^{-1}. Drifter results from the diversion suggest that the wastewater plume was transported at velocities typically between 5 and 15 cm s^{-1}, with approximately equal transport up-coast and down-coast (Rogowski et al. 2014). For this exercise, we assume complete and uniform mixing over the course of a single day in the

theoretical box of approximately 12 km^3, whose dimensions were generated by the observed velocities (assuming equal distances in x and y of 17.28 km, from velocities of 10 cm s^{-1} for 24 hours in all directions, over a depth horizon, z, of 40 m). We assumed a "normal operations" subeuphotic average nitrification rate of 80 nmol L^{-1} d^{-1}, which was the average of subeuphotic nitrification rates at 2205 pre-diversion and 2207 post-diversion, both areas registering the highest proximity to the effluent plume track and thus considered to be indicative of minimally diluted effluent plume, and a during-diversion rate of 34 nmol L^{-1} d^{-1}, which was the average of values at stations 2205, 2207 and 2208, areas indicative of minimal plume activity. Using these rates, we calculated the amount of ammonium oxidized in this box while the deep outfall pipe was operating and compared to when it was out of service. When the deep outfall was operational, 9.6×10^8 moles of NH$_4^+$ per day would have been oxidized in this box, whereas during-diversion (deep outfall off), 4.1×10^8 moles of NH$_4^+$ would have been oxidized. The difference between the two time points, 5.5×10^8 moles of NH$_4^+$, is the same order of magnitude as the amount of ammonium discharged from the OCSD outfall, 9.3×10^8 moles of NH$_4^+$ per day, assuming an average concentration of NH$_4^+$ in the effluent of 1740 µM (Table 1). This analysis implies that "background" nitrification rates (represented by the during-diversion time point), were increased up to 3-fold due to the presence of wastewater ammonium and that wastewater ammonium was a significant source of new nitrate to the euphotic zone during normal operations. It also implies that a lack of measured ammonium in the far-field was not necessarily evidence of a lack or dilution of wastewater nitrogen in the region. However, these are simple "back of the envelope" calculations and to fully understand the impact of wastewater on nitrogen cycling would require an intensive modeling endeavor.

4.3. Nitrified-N was incorporated into the biomass

Stable isotope ratios of particulate organic matter (POM) indicate the incorporation of nitrified ammonium into bacteria and phytoplankton around the outfall. The low values in suspended particulate $\delta^{15}N_{PN}$ and $\delta^{13}C_{PN}$ within the plume (Figure 3b) suggested that newly-nitrified NO_3^- and wastewater dissolved organic carbon (DOC) was being incorporated into the biomass. Given that NH_4^+ concentrations around the deep outfall were relatively high, nitrification could result in a strong isotopic discrimination. In this case $^{14}NH_4^+$ was favored for oxidation, resulting in an initially low $\delta^{15}N_{NO3}$. This would, in turn, be preferentially incorporated into the biomass (assimilation favoring $^{14}NO_3^-$), leaving the residual $\delta^{15}N_{NO3}$ pool enriched and explaining observed higher $\delta^{15}N_{NO3}$ values near the outfall. As ammonium becomes scarce away from the outfall, the discrimination becomes less and the biomass becomes more isotopically enriched. Additionally, anthropogenic DOC typically has a lower $\delta^{13}C_{PN}$ relative to other carbon sources (e.g., marine phytoplankton) (Wang et al. 1998, Griffith et al. 2009), which may account for the lower signature around the deep outfall as heterotrophic bacteria utilize the DOC in the wastewater stream as a carbon substrate for growth (see Caron et al., this issue). This was consistent with the low suspended particulate C:N ratios observed (Goldman et al. 1987).

The isotopic discrimination calculated for nitrification in wastewater was consistent with the low values in $\delta^{15}N_{PN}$, a further line of evidence that nitrified-ammonium was making its way into bacteria and phytoplankton biomass near outfalls. Ammonium concentrations were high around the deep outfall and thus a value for the isotopic composition of water column NH_4^+ could be measured (analysis was limited due to the fact that roughly 2 μmoles of ammonium is

required for isotope analysis (Holmes et al. 1998)). Values for water column ammonium were slightly less than the $\delta^{15}N_{NH4}$ measured in wastewater effluent (Table 1) and higher than the average water column $\delta^{15}N_{PN}$ and $\delta^{15}N_{NO3}$ (Table 2), which suggests that most of the water column ammonium was sourced from wastewater. The difference between the isotopic composition of wastewater nitrate and ammonium may reflect the isotopic discrimination during nitrification during the wastewater treatment process. This isotope effect can be calculated assuming Rayleigh fractionation (Mariotti et al. 1981):

$$\delta^{15}N_{NO3} = \delta^{15}N_{NH4\ initial} + \epsilon_{nit} * f_{NH4} * (\ln[f_{NH4}]/[1-f_{NH4}]) \qquad \text{(Eq. 5)}$$

$$f_{NH4} = [NH_4^+]_{observed} / [DIN]_{observed} \qquad \text{(Eq. 6)}$$

Where f_{NH4} is the residual fraction of ammonium remaining in the dissolved inorganic nitrogen (DIN) pool, and $[NH_4^+]_{observed}$ and $[DIN]_{observed}$ are the ammonium and DIN concentrations in the effluent sample respectively. Rearranging Eq. 5, you can solve for the isotope effect ϵ_{nit}:

$$\epsilon_{nit} = (\delta^{15}N_{NH4\ initial} - \delta^{15}N_{NO3})/ (f_{NH4} * (\ln[f_{NH4}]/[1-f_{NH4}]) \qquad \text{(Eq. 7)}$$

Using the average effluent concentrations for nitrate and ammonium from Table 1 yields an f_{NH4} of 0.72 and a ϵ_{nit} of -8.84. This isotope effect was consistent with the low $\delta^{15}N_{PN}$ values observed near the outfall pipes which were on the order of 10‰ lower than effluent $\delta^{15}N_{NH4}$, suggesting that PN was incorporating nitrified effluent ammonium.

Stable isotopic evidence from net tows suggests the trophic transfer of nitrogen and carbon from the microbial and phytoplankton communities into higher levels of the foodweb (Figure 6). Stable isotope ratios are often used to determine the trophic status of organisms (Layman et al. 2007, Boecklen et al. 2011), and, while a comprehensive analysis of trophic

structure on the San Pedro Shelf was beyond the scope of this study, we did characterize the stable isotopic composition (δ^{15}N and δ^{13}C) of samples collected in two net tows (20 μm and 200 μm) to investigate if nitrified ammonium from discharges was incorporated into grazer communities. The δ^{15}N and δ^{13}C values of the 20 μm and 200 μm net tows were typically higher than the particulate material collected on a GF/F filter (by between 1 to 5 ‰ for δ^{15}N and between 0.5 and 2.5 ‰ for δ^{13}C, Figure 6), which may be indicative of trophic transfer of nutrients from microbial cycling and primary producers to grazer communities. These trophic fractionations were similar in magnitude to what has been observed as trophic step fractionations in other aquatic ecosystems (Keough et al. 1996, Post 2002, Fredriksen 2003, Dubois et al. 2007). More research is needed to fully map the importance of anthropogenic nitrogen on foodwebs around ocean outfalls, but this preliminary dataset suggests that nitrogen sourced from the outfalls may be transferred to grazer communities in the SCB.

4. Implications for Coastal Eutrophication.

Eutrophication in the SCB is a controversial issue because the historical perception has been that coastal upwelling regions are less impacted by, and more resilient to, anthropogenic nutrient inputs. However, several recent studies have provided evidence to the contrary, and researchers have begun to question the resilience of these systems (Capone and Hutchins 2013). Wastewater effluent has been shown to provide an equivalent flux of N as 'natural' sources (i.e. upwelling) in the urbanized regions of the SCB which has additional implications for the dominant form of N (Howard et al. 2014). The extent of algal blooms in the SCB have increased significantly over the last decade, with chronic blooms documented in areas of the

SCB co-located with major inputs of anthropogenic nutrients (Schnetzer et al. 2007, Nezlin et al. 2012, Schnetzer et al. 2013). Furthermore, anthropogenic N has been implicated as a potential cause for algal blooms, particularly harmful algal blooms (HABs) (Anderson et al. 2002, Kudela et al. 2008, Reifel et al. 2013). In addition, analysis of a decade of quarterly ocean surveys across the central and northern SCB have shown a significant decrease in dissolved oxygen (DO) concentrations and that the rate of the DO decline in the nearshore, proximal to wastewater outfalls, was greater than offshore regions (Booth et al. 2014), and acute hypoxic events have been seen in estuaries and harbors (Stauffer et al. 2013). Given these trends, it is critical to have a better understanding of the effects of anthropogenic nutrients on biological productivity, and coastal hypoxia.

Isotopic evidence from this study suggests incorporation of "new" N from oxidized wastewater ammonium into the biomass. While wastewater effluent has traditionally been ignored as a significant N source in the SCB, several studies conducted in close proximity to large wastewater discharges have concluded that classical coastal upwelling does not always drive nearshore chlorophyll and productivity (Kim et al. 2009, Corcoran and Shipe 2011, Nezlin et al. 2012). Given that wastewater effluent can contribute up to half of N in the urbanized areas of the SCB in the form of ammonium (Howard et al. 2014), the results from this study suggest that nitrification of wastewater effluent ammonium can provide a significant source of nitrate to the shelf.

Our results contribute to an evolving conceptual model for how anthropogenic nutrients may affect coastal ocean biogeochemistry in urban settings. In the SCB, wastewater enters the

ocean predominantly as ammonium, which is rapidly oxidized to nitrate in proximity to the outfalls. The isotopic composition of suspended particulate matter suggests incorporation of this "new" N from oxidized wastewater ammonium into the biomass. However, given the low productivity throughout the study period, more work should be conducted to evaluate the relative importance of this source of N and its effect on coastal eutrophication in the SCB.
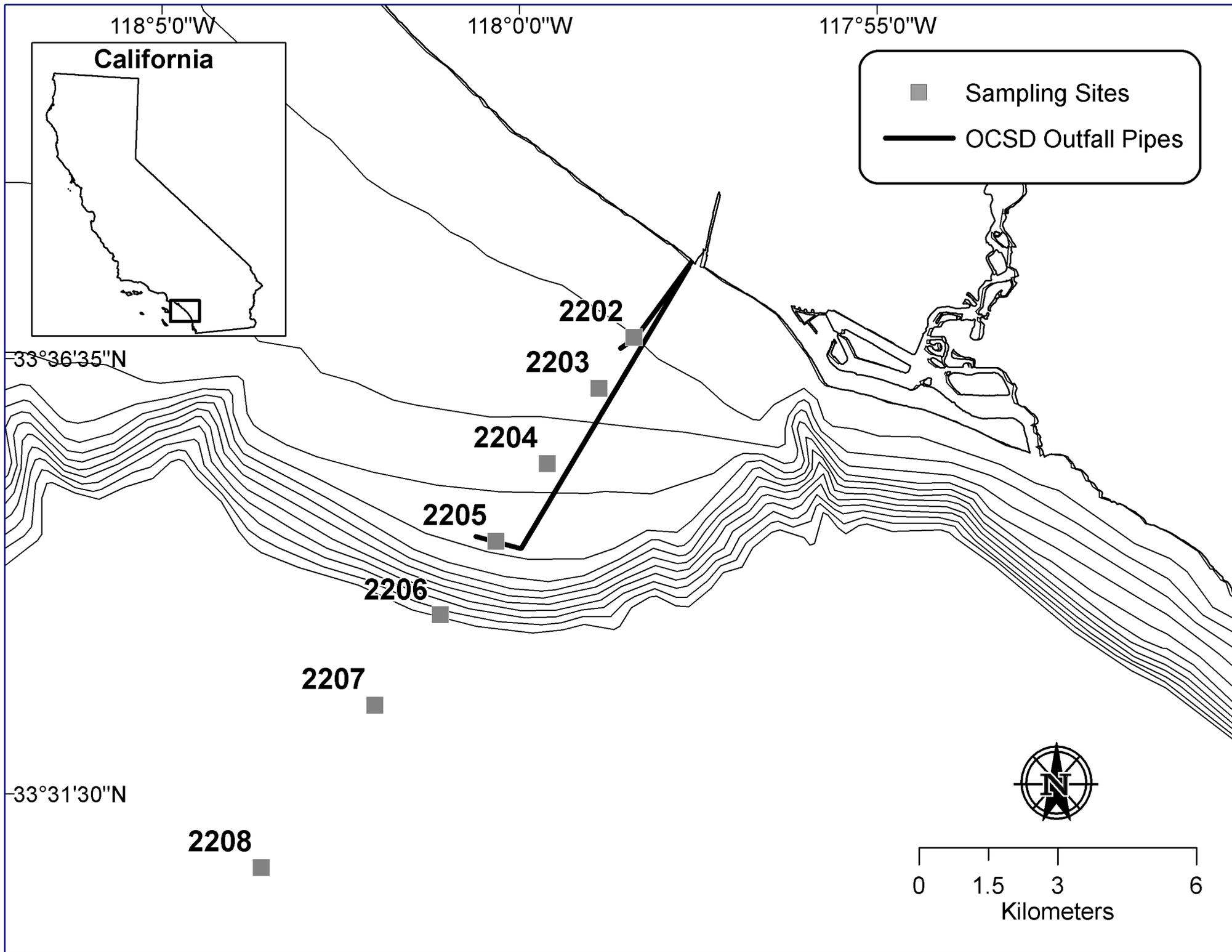
Acknowledgements

References

Anderson, D. M., P. M. Glibert, and J. M. Burkholder. 2002. Harmful algal blooms and eutrophication: Nutrient sources, composition, and consequences. Estuaries **25**:704-726.
Boecklen, W. J., C. T. Yarnes, B. A. Cook, and A. C. James. 2011. On the use of stable isotopes in trophic ecology. Annual Review of Ecology, Evolution, and Systematics **42**:411-440.
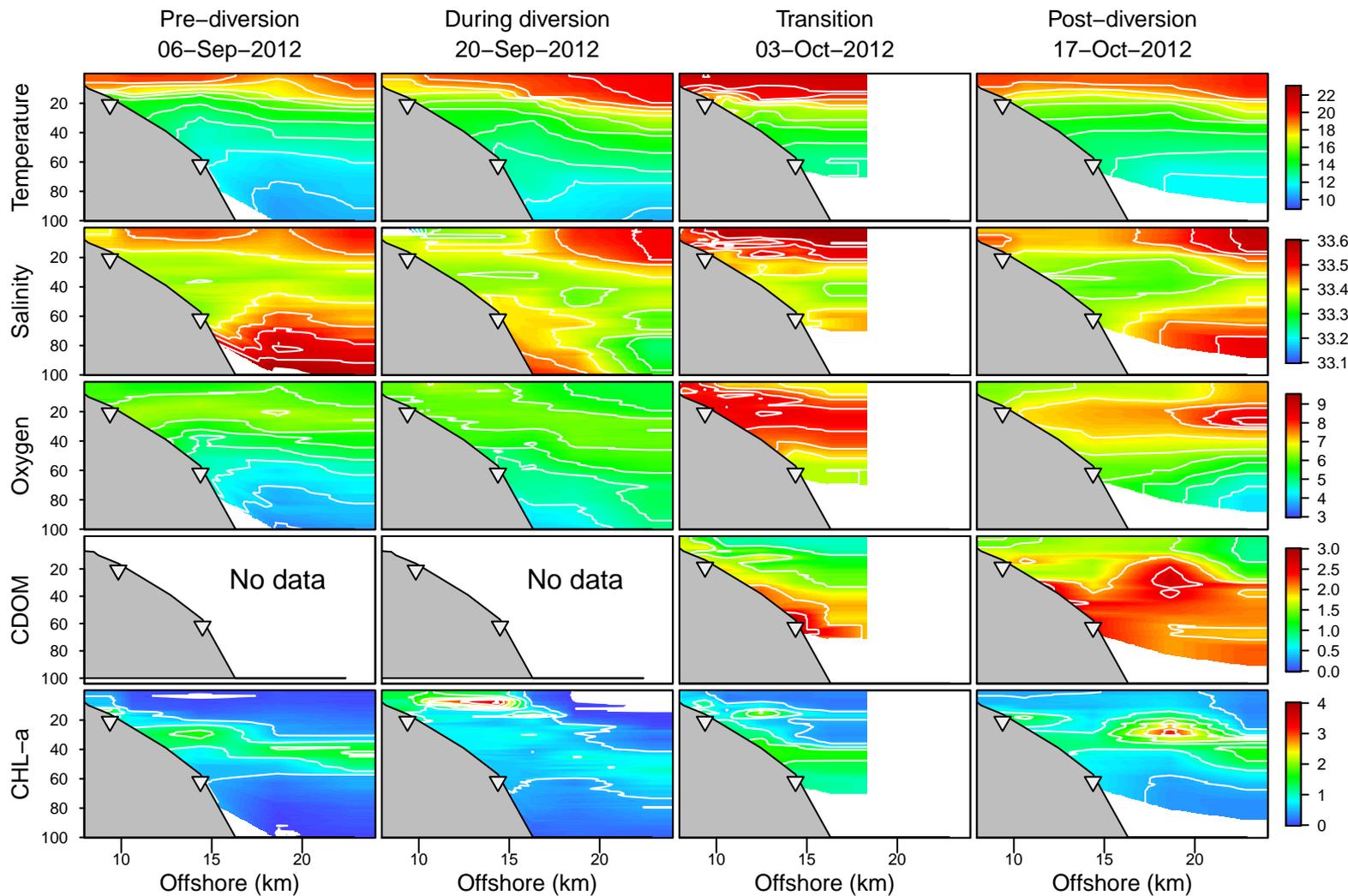
Booth, J. A. T., C. B. Woodson, M. Sutula, F. Micheli, S. B. Weisberg, S. J. Bograd, A. Steele, J. Schoen, and L. B. Crowder. 2014. Patterns and potential drivers of declining oxygen content along the southern california coast. Limnology and Oceanography **59**:1127-1138.

Boss, E., W. S. Pegau, J. R. V. Zaneveld, and A. H. Barnard. 2001. Spatial and temporal variability of absorption by dissolved material at a continental shelf. Journal of Geophysical Research: Oceans (1978–2012) **106**:9499-9507.

Brandes, J. A., A. H. Devol, T. Yoshinari, D. A. Jayakumar, and S. W. A. Naqvi. 1998. Isotopic composition of nitrate in the central arabian sea and eastern tropical north pacific: A tracer for mixing and nitrogen cycles. Limnology & Oceanography **43**:1680-1689.

Capone, D. G. and D. A. Hutchins. 2013. Microbial biogeochemistry of coastal upwelling regimes in a changing ocean. Nature Geoscience **6**:711-717.

Casciotti, K. L., D. M. Sigman, M. G. Hastings, J. K. Bohlke, and A. Hilkert. 2002. Measurement of the oxygen isotopic composition of nitrate in seawater and freshwater using the denitrifier method. Analytical Chemistry **74**:4905-4912.

Chavez, F. P. and M. Messié. 2009. A comparison of eastern boundary upwelling ecosystems. Progress in Oceanography **83**:80-96.

Corcoran, A. A. and R. F. Shipe. 2011. Inshore-offshore and vertical patterns of phytoplankton biomass and community composition in santa monica bay, ca (USA). Estuarine Coastal and Shelf Science **94**:24-35.

Cullen, J. and R. Eppley. 1981. Chlorophyll maximum layers of the southern-california bight and possible mechanisms of their formation and maintenance. Oceanologica Acta **4**:23-32.

Deutsch, C., N. Gruber, R. M. Key, J. L. Sarmiento, and A. Ganachaud. 2001. Denitrification and n-2 fixation in the pacific ocean. Global Biogeochemical Cycles **15**:483-506.

Dubois, S., B. Jean-Louis, B. Bertrand, and S. Lefebvre. 2007. Isotope trophic-step fractionation of suspension-feeding species: Implications for food partitioning in coastal ecosystems. Journal of Experimental Marine Biology and Ecology **351**:121-128.

Fredriksen, S. 2003. Food web studies in a norwegian kelp forest based on stable isotope (delta^ 1^ 3c and delta^ 1^ 5n) analysis. MARINE ECOLOGY-PROGRESS SERIES- **260**:71-81.

Goeyens, L., Kindermans, N., Abu Yusuf, M., Elskens, M. 1998. A room temperature procedure for the manual determination of urea in seawater. Estaurine, Coastal and Shelf Science **47**:415-418.

Goldman, J. C., D. A. Caron, and M. R. Dennett. 1987. Regulation of gross growth efficiency and ammonium regeneration in bacteria by substrate c-n ratio. Limnology and Oceanography **32**:1239-1252.

Granger, J., D. M. Sigman, J. A. Needoba, and P. J. Harrison. 2004. Coupled nitrogen and oxygen isotope fractionation of nitrate during assimilation by cultures of marine phytoplankton. Limnology and Oceanography **49**:1763-1773.

Griffith, D. R., R. T. Barnes, and P. A. Raymond. 2009. Inputs of fossil carbon from wastewater treatment plants to us rivers and oceans. Environmental Science & Technology **43**:5647-5651.

Gruber, N. and J. L. Sarmiento. 1997. Global patterns of marine nitrogen fixation and denitrification. Global Biogeochemical Cycles **11**:235-266.

Hannon, J. E. and J. K. Böhlke. 2008. Determination of the δ(15n/14n) of ammonium (nh4+) in water: Rsil lab code 2898, chap. C15. Page 30 *in* K. Révész and T. B. Coplen, editors. Methods of the reston stable isotope laboratory: U.S. Geological survey, techniques and methods, Reston, VA.

Henriksen, K. 1988. Nitrification in estuarine and coastal marine sediments. Nitrogen cycling in coastal marine environments.

Holmes, R. M., A. Aminot, R. Kerouel, B. A. Hooker, and B. J. Peterson. 1999. A simple and precise method for measuring ammonium in marine and freshwater ecosystems. Canadian Journal of Fisheries and Aquatic Sciences **56**:1801-1808.
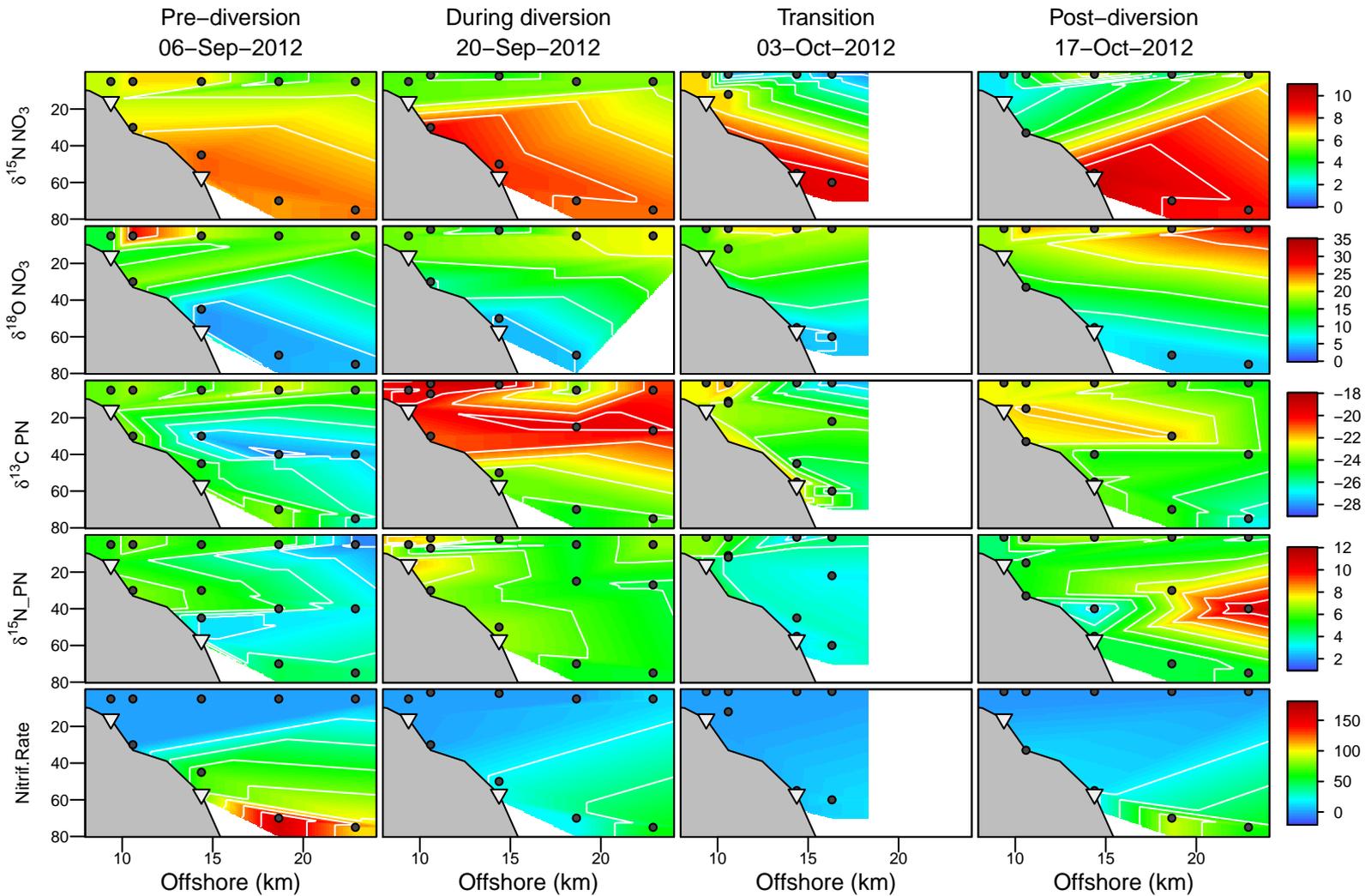
Holmes, R. M., J. W. McClelland, D. M. Sigman, B. Fry, and B. J. Peterson. 1998. Measuring n-15-nh4+ in marine, estuarine and fresh waters: An adaptation of the ammonia diffusion method for samples with low ammonium concentrations. Marine Chemistry **60**:235-243.

Howard, M. D. A., G. Robertson, M. Sutula, B. Jones, N. Nezlin, Y. Chao, H.Frenzel, M. Mengel, D. A. Caron, B.Seegers, A. Sengupta, E. Seubert, D. Diehl, and S. B. Weisberg. 2012. Southern california bight 2008 regional monitoring program: Volume vii. Water quality. Technical report 710. . Southern California Coastal Water Research Project. Costa Mesa, CA.

Howard, M. D. A., M. Sutula, D. A. Caron, Y. Chao, J. D. Farrara, H. Frenzel, B. Jones, G. Robertson, K. McLaughlin, and A. Sengupta. 2014. Anthropogenic nutrient sources rival natural sources on small scales in the coastal waters of the southern california bight. Limnology and Oceanography **59**:285-297.

Howarth, R. W. and R. Marino. 2006. Nitrogen as the limiting nutrient for eutrophication in coastal marine ecosystems: Evolving views over three decades. Limnology and Oceanography **51**:364-376.

Kendall, C. 1998. Tracing nitrogen sources and cycling in catchments. Pages 519-576 *in* C. Kendall and J. J. McDonnell, editors. Isotope tracers in catchment hydrology. Elsevier Science B.V., Amsterdam.

Keough, J. R., M. E. Sierszen, and C. A. Hagley. 1996. Analysis of a lake superior coastal food web with stable isotope techniques. Limnology and Oceanography **41**:136-146.

Kim, H.-J., A. J. Miller, J. McGowan, and M. L. Carter. 2009. Coastal phytoplankton blooms in the southern california bight. Progress in Oceanography **82**:137-147.

Kudela, R. M., J. Q. Lane, and W. P. Cochlan. 2008. The potential role of anthropogenically derived nitrogen in the growth of harmful algae in california, USA. Harmful Algae **8**:103-110.

Layman, C. A., D. A. Arrington, C. G. Montaña, and D. M. Post. 2007. Can stable isotope ratios provide for community-wide measures of trophic structure? Ecology **88**:42-48.

Lipschultz, F., S. C. Wofsy, B. B. Ward, L. A. Codispoti, G. Friedrich, and J. W. Elkins. 1990. Bacterial transformations of inorganic nitrogen in the oxygen-deficient waters of the eastern tropical south-pacific ocean. Deep-Sea Research Part a-Oceanographic Research Papers **37**:1513-+.

Lyon, G. S. and E. D. Stein. 2009. How effective has the clean water act been at reducing pollutant mass emissions to the southern california bight over the past 35 years? Environmental Monitoring and Assessment **154**:413-426.

Mariotti, A., J. Germon, P. Hubert, P. Kaiser, R. Letolle, A. Tardieux, and P. Tardieux. 1981. Experimental determination of nitrogen kinetic isotope fractionation: Some principles; illustration for the denitrification and nitrification processes. Plant and Soil **62**:413-430.

Nezlin, N., M. A. Sutula, R. P. Stumpf, and A. Sengupta. 2012. Phytoplankton blooms detected by seawifs along the central and southern california coast. Journal of Geophsical Research **117**:C07004.

Patton, C. and J. R. Kryskalla. 2003. Methods of analysis by the u.S. Geological survey national water quality laboratory—evaluation of alkaline persulfate digestion as an alternative to kjeldahl digestion for determination of total and dissolved nitrogen and phosphorus in water, water-resources investigations report 03–4174. U.S. Department of the Interior, U.S. Geological Survey, Denver, CO.

Post, D. M. 2002. Using stable isotopes to estimate trophic position: Models, methods, and assumptions. Ecology **83**:703-718.

Prairie, Y. T., R. H. Peters, and D. F. Bird. 1995. Natural variability and the estimation of empirical relationship: A reassessment of regression methods. Canadian Journal of Fishery and Aquatic Sciences **52**:788-798.

Reifel, K. M., A. A. Corcoran, C. Cash, R. Shipe, and B. H. Jones. 2013. Effects of a surfacing effluent plume on a coastal phytoplankton community. Continental Shelf Research **60**:38-50.
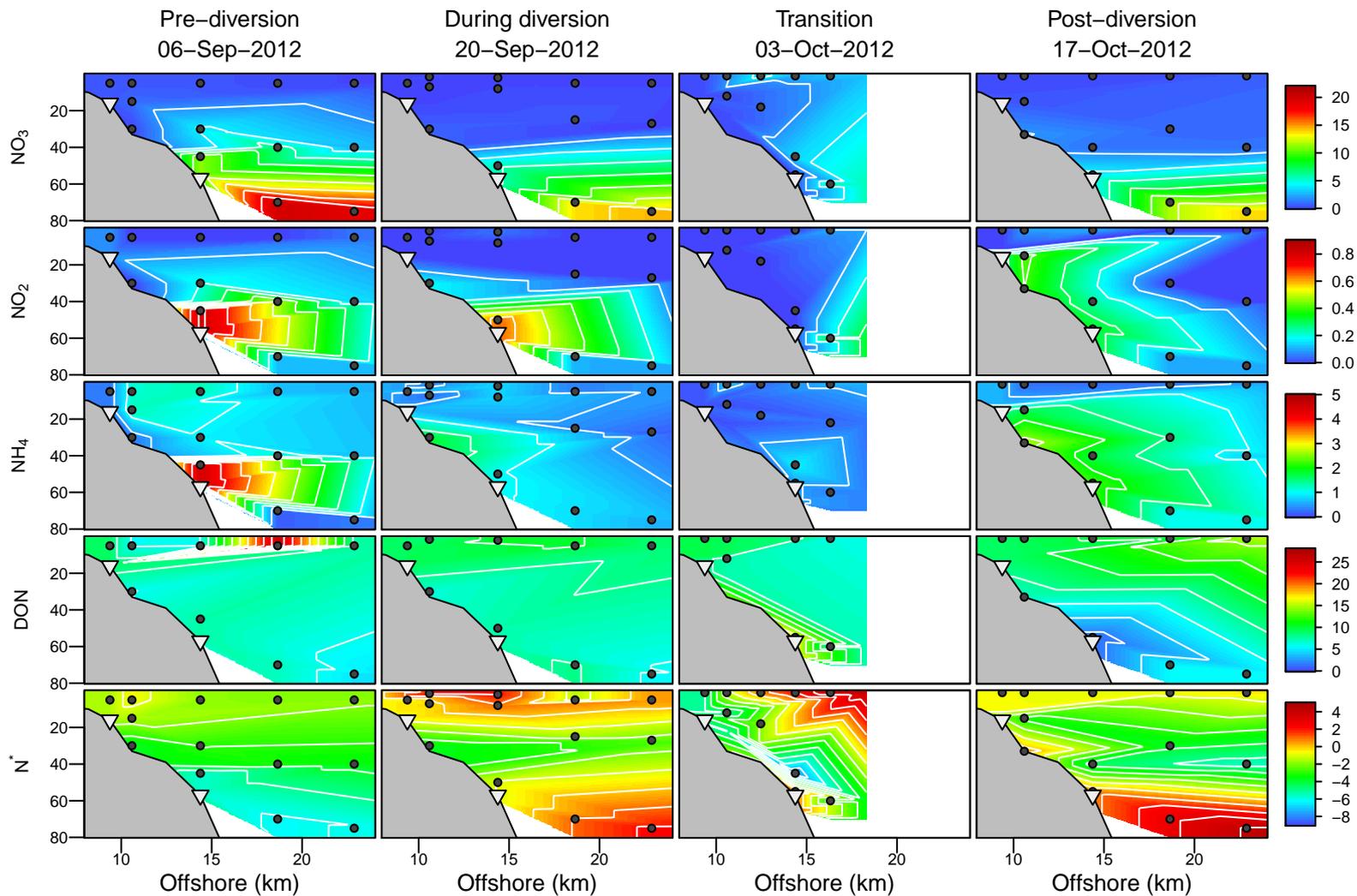
Rogowski, P., E. Terrill, M. P. Otero, L. Hazard, and W. Middleton. 2012. Mapping ocean outfall plumes and their mixing using autonomous underwater vehicles. Journal of Geophysical Research-Oceans **117** 1-12.

Rogowski, P., E. Terrill, M. P. Otero, L. Hazard, and W. Middleton. 2013. Ocean outfall plume characterization using an autonomous underwater vehicle. Water Science and Technology **67**:925-933.

Rogowski, P., E. Terrill, J. Thomas, L. Rosenfeld, and J. Largier. 2014. 2012 orange county sanitation district (ocsd) outfall diversion–summary report. Final report prepared for the orange county sanitation district. March 25, 2014.

Santoro, A. E., K. L. Casciotti, and C. A. Francis. 2010a. Activity, abundance and diversity of nitrifying archaea and bacteria in the central california current. Environmental Microbiology **12**:1989-2006.

Santoro, A. E., N. J. Nidzieko, G. L. van Dijken, K. R. Arrigo, and A. B. Boehm. 2010b. Contrasting spring and summer phytoplankton dynamics in the nearshore southern california bight. Limnology and Oceanography **55**:264-278.

Schnetzer, A., B. H. Jones, R. A. Schaffner, I. Cetinic, E. Fitzpatrick, P. E. Miller, E. L. Seubert, and D. A. Caron. 2013. Coastal upwelling linked to toxic pseudo-nitzschia australis blooms in los angeles coastal waters, 20052007. Journal of Plankton Research **35**:1080-1092.

Schnetzer, A., P. E. Miller, R. A. Schaffner, B. A. Stauffer, B. H. Jones, S. B. Weisberg, P. M. DiGiacomo, W. M. Berelson, and D. A. Caron. 2007. Blooms of pseudo-nitzschia and domoic acid in the san pedro channel and los angeles harbor areas of the southern california bight, 2003-2004. Harmful Algae **6**:372-387.

Sigman, D. M., J. Granger, P. J. DiFiore, M. M. Lehmann, R. Ho, G. Cane, and A. van Geen. 2005. Coupled nitrogen and oxygen isotope measurements of nitrate along the eastern north pacific margin. Global Biogeochemical Cycles **19**.

Sigman, D. M., R. Robinson, A. N. Knapp, A. van Geen, D. C. McCorkle, J. A. Brandes, and R. C. Thunell. 2003. Distinguishing between water column and sedimentary denitrification in the santa barbara basin using the stable isotopes of nitrate. Geochemistry Geophysics Geosystems **4**.

Stauffer, B. A., A. Schnetzer, A. G. Gellene, C. Oberg, G. S. Sukhatme, and D. A. Caron. 2013. Effects of an acute hypoxic event on microplankton community structure in a coastal harbor of southern california. Estuaries and Coasts **36**:135-148.

Sugimoto, R., A. Kasai, T. Miyajima, and K. Fujita. 2009. Controlling factors of seasonal variation in the nitrogen isotope ratio of nitrate in a eutrophic coastal environment. Estuarine Coastal and Shelf Science **85**:231-240.

Thomas, W. H., D. L. Seibert, and A. N. Dodson. 1974. Phytoplankton enrichment experiments and bioassays in natural coastal sea water and in sewage outfall receiving waters off southern california. Estuarine and Coastal Marine Science **2**:191-206.

Wang, Y., T. G. Huntington, L. J. Osher, L. I. Wassenaar, S. E. Trumbore, R. G. Amundson, J. W. Harden, D. M. McKnight, S. L. Schiff, G. R. Aiken, W. B. Lyons, R. O. Araavena, and J. S. Baron. 1998. Carbon cycling in terrestrial environments. Pages 577-610 *in* C. Kendall and J. J. McDonnell, editors. Isotope tracers in catchment hydrology. Elsevier Science.

Wankel, S. D., C. Kendall, C. A. Francis, and A. Paytan. 2006. Nitrogen sources and cycling in the san francisco bay estuary: A nitrate dual isotopic composition approach. Limnology and Oceanography **51**:1654-1664.

Wankel, S. D., C. Kendall, J. T. Pennington, F. P. Chavez, and A. Paytan. 2007. Nitrification in the euphotic zone as evidenced by nitrate dual isotopic composition: Observations from monterey bay, california. Global Biogeochemical Cycles **21**.

Ward, B. B. 1987a. Nitrogen transformations in the southern-california bight. Deep-Sea Research Part a-Oceanographic Research Papers **34**:785-805.

Ward, B. B. 1987b. Nitrogen transformations in the southern california bight. Deep-Sea Reseach **34**:785-805.

Ward, B. B. 2005. Temporal variability in nitrification rates and related biogeochemical factors in monterey bay, california, USA. Marine Ecology Progress Series **292**:97-109.

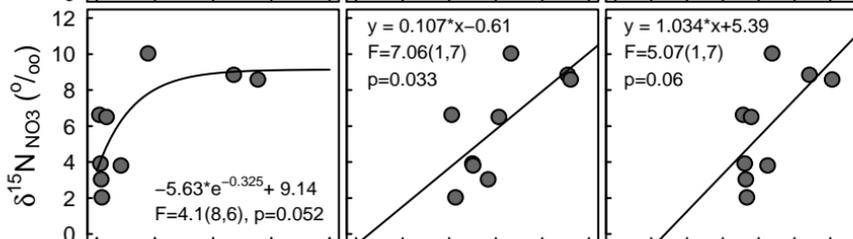Figure: Cross-shore distributions of $\delta^{15}N$ NO_3, $\delta^{18}O$ NO_3, $\delta^{13}C$ PN, $\delta^{15}N\_PN$, and Nitrif.Rate for four periods: Pre-diversion (06-Sep-2012), During diversion (20-Sep-2012), Transition (03-Oct-2012), and Post-diversion (17-Oct-2012). X-axis: Offshore (km); Y-axis: depth.

Figure showing δ¹⁵N_NO3 (‰) plotted against NO₃ (μM), NO₃ (%), and N* for four dates in 2012.

Row 06-Sep-2012:
- $-2.37*e^{-1.04} + 7.71$; $F=4.7(8,6)$, $p=0.038$
- $y = 0.024*x + 5.39$; $F=5.47(1,7)$, $p=0.05$
- $y = -0.348*x + 5.52$; $F=6.71(1,7)$, $p=0.04$

Row 20-Sep-2012:
- $-5.76*e^{-3.75} + 8.24$; $F=27.9(8,6)$, $p=0.000$
- $y = 0.035*x + 4.83$; $F=5.39(1,7)$, $p=0.05$
- $y = -0.382*x + 6.58$; $F=1.73(1,7)$, $p=0.23$

Row 03-Oct-2012:
- $12.4*e^{-3.01} + 3.55$; $F=1.2(6,4)$, $p=0.465$
- $y = -0.084*x + 11.77$; $F=0.94(1,5)$, $p=0.38$
- $y = -0.556*x + 4.71$; $F=2.07(1,5)$, $p=0.21$

Row 17-Oct-2012:
- $-5.63*e^{-0.325} + 9.14$; $F=4.1(8,6)$, $p=0.052$
- $y = 0.107*x - 0.61$; $F=7.06(1,7)$, $p=0.033$
- $y = 1.034*x + 5.39$; $F=5.07(1,7)$, $p=0.06$

X-axis labels: NO_3 (μM), NO_3 (%), N^*
Y-axis label: $\delta^{15}N_{NO3}$ (‰)